Title

Influence of Vacuum Cooling on Escherichia coli O157:H7 Infiltration in Fresh Leafy Greens via a Multiphoton-Imaging Approach

Journal

Applied and Environmental Microbiology, 82(1)

ISSN

0099-2240

Authors

Vonasek, Erica
Nitin, Nitin

Publication Date

2016

DOI

10.1128/aem.02327-15

Peer reviewed

AMERICAN SOCIETY FOR MICROBIOLOGY | Applied and Environmental Microbiology

Influence of Vacuum Cooling on *Escherichia coli* O157:H7 Infiltration in Fresh Leafy Greens via a Multiphoton-Imaging Approach

Erica Vonasek,[a] Nitin Nitin[a,b]

Department of Biological and Agricultural Engineering[a] and Department of Food Science & Technology,[b] University of California, Davis, Davis, California, USA

Microbial pathogen infiltration in fresh leafy greens is a significant food safety risk factor. In various postharvest operations, vacuum cooling is a critical process for maintaining the quality of fresh produce. The overall goal of this study was to evaluate the risk of vacuum cooling-induced infiltration of *Escherichia coli* O157:H7 into lettuce using multiphoton microscopy. Multiphoton imaging was chosen as the method to locate *E. coli* O157:H7 within an intact lettuce leaf due to its high spatial resolution, low background fluorescence, and near-infrared (NIR) excitation source compared to those of conventional confocal microscopy. The variables vacuum cooling, surface moisture, and leaf side were evaluated in a three-way factorial study with *E. coli* O157:H7 on lettuce. A total of 188 image stacks were collected. The images were analyzed for *E. coli* O157:H7 association with stomata and *E. coli* O157:H7 infiltration. The quantitative imaging data were statistically analyzed using analysis of variance (ANOVA). The results indicate that the low-moisture condition led to an increased risk of microbial association with stomata ($P < 0.05$). Additionally, the interaction between vacuum cooling levels and moisture levels led to an increased risk of infiltration ($P < 0.05$). This study also demonstrates the potential of multiphoton imaging for improving sensitivity and resolution of imaging-based measurements of microbial interactions with intact leaf structures, including infiltration.

Vacuum cooling is a postharvest-processing operation that preserves the quality of fresh produce by rapidly reducing its temperature. Cooling fresh produce to refrigerated temperatures increases shelf life and product quality by reducing cellular activity (1). The vacuum cooling process cools fresh produce by lowering pressure within a sealed chamber and inducing surface moisture evaporation (2–5). Evaporating the surface moisture reduces the enthalpy in the system by taking energy from the surrounding tissue, thereby reducing the temperature in fresh produce. The product may be sprayed with water during the vacuum cooling process in order to prevent excessive water loss from surface evaporation (4, 5).

A recent study suggested that vacuum cooling may increase the risk of microbial infiltration into fresh produce, thereby increasing the risk of food-borne illness from microbial food pathogens (6). Microbial infiltration of pathogens in fresh leafy greens significantly increases the risk of food-borne illness, as the infiltrated microbes cannot be effectively removed or treated utilizing standard sanitation and washing processes (6, 7). Microbial infiltration has been reported in both preharvest and postharvest processing of leafy greens (7, 8). During postharvest, microbial infiltration mechanisms are predominantly associated with stomata in intact leaf tissue and in some cases associated with damage to the leaf tissue due to the presence of nutrients from these openings in the plant tissue (6–9). Thus, the reported increase in microbial infiltration as a result of vacuum cooling operations is a serious concern. To confirm the risk of microbial infiltration due to vacuum cooling, the method to determine infiltration and the commonly used parameters in the fresh-produce industry need further examination.

One of the key challenges in establishing the microbial infiltration of plant tissue is to distinguish between microbes on the surface of a plant and microbes that have infiltrated the plant tissue (6, 7). Optical microscopy techniques, such as fluorescence confocal microscopy, are often used for these measurements. However, there are significant challenges in imaging plant leaves using conventional confocal microscopy (6). These challenges result from the heterogeneous topology of the plant surface, extensive scattering of excitation light in the plant matrix, and significant endogenous fluorescence of plant leaves in the wavelengths commonly used for confocal microscopy (10). The surface topology of plant leaves is highly heterogeneous, with micron-scale variations. The extensive scattering of visible excitation light on leafy greens further reduces the ability of confocal microscopy to resolve fluorescent signal to detect microbes (11). Furthermore, the broad endogenous fluorescence in plant leaves due to native chromophores, such as chlorophyll, results in significant amounts of background fluorescence (12). The background fluorescence of plant leaves limits and confounds the detection of fluorescently tagged microbes. Thus, both the structural and compositional features of the plant leaves significantly reduce the spatial resolution and the sensitivity of detection using conventional confocal microscopy, and they introduce confounding background artifacts.

Multiphoton microscopy is proposed as an alternative to address the limitations of using confocal microscopy to detect fluorescent microbes on and within plant tissue. The unique advantages of multiphoton microscopy compared to standard confocal microscopy are that (i) near-infrared (NIR) wavelength of excitation light in multiphotons significantly reduces the scattering and

Received 21 July 2015 **Accepted** 12 October 2015

Accepted manuscript posted online 16 October 2015

Citation Vonasek E, Nitin N. 2016. Influence of vacuum cooling on *Escherichia coli* O157:H7 infiltration in fresh leafy greens via a multiphoton-imaging approach. Appl Environ Microbiol 82:106–115. doi:10.1128/AEM.02327-15.

Editor: D. W. Schaffner

Address correspondence to Nitin Nitin, nnitin@ucdavis.edu.

Supplemental material for this article may be found at http://dx.doi.org/10.1128/AEM.02327-15.

increases the depth of penetration and (ii) the nonlinear combination of pulsed-laser excitation sources significantly reduces the out-of-focus excitation compared to that with conventional confocal microscopy (13–15). This approach has a significant advantage in reducing the background autofluorescence of plant leaves and can significantly enhance the sensitivity of detection of microbes and reduce contributions from confounding plant microstructures (16). Despite the significant advantages of multiphoton microscopy, this approach has not been extensively used in plant research, especially to map potential changes in the localization of microbes induced by postharvest processing of leafy greens.

This study evaluates the risk of vacuum cooling inducing microbial infiltration in lettuce leaves using multiphoton microscopy. *Escherichia coli* O157:H7 was used as a representative microbial pathogen in this study. The conditions of (i) vacuum cooling treatment, (ii) surface moisture, and (iii) leaf surfaces, either abaxial (bottom) or adaxial (top), were evaluated to understand the potential factors influencing infiltration. By identifying and evaluating the key conditions that can be optimized in a cooling operation, recommendations for reducing microbial infiltration in fresh produce through the vacuum cooling process can be made.

MATERIALS AND METHODS

Development of *E. coli* O157:H7 GFPlux. *E. coli* O157:H7 GFPlux was used in all experiments. *E. coli* O157:H7 (ATCC 700728) was a gift from Maria Marco (University of California, Davis, CA). The pAKgfplux1 plasmid was a gift from Attila Karsi (Addgene plasmid 14083) and is a low-copy-number plasmid with constitutive expression of green fluorescent protein (GFP), with a 488-nm excitation/500- to 550-nm emission, bacterial luciferase (LuxCDABE), and ampicillin resistance (17). *E. coli* O157:H7 was transformed by heat shock with the pAKgfplux1 plasmid. Briefly, pAKgfplux1 was purified from the *E. coli* DH5α host using the PureLink quick plasmid miniprep kit (Invitrogen). *E. coli* O157:H7 cells were made competent by use of the Single Step Ultra-Competent cell preparation kit (BioPioneer, Inc.) and transformed with the plasmid through heat shock. The transformed cells were then incubated with LB for 1 h and plated on 100 μg/ml ampicillin LB agar plates for overnight incubation at 37°C. After a single colony was picked and cultured in a liquid LB medium with 100 μg/ml ampicillin until the optical density (OD) at 600 nm reached 1.0, the liquid culture was assayed for fluorescence and luminescence signal using a plate reader and a fluorescence imaging microscope in comparison to *E. coli* BL21, which was not modified to be fluorescent or bioluminescent. After confirmation that both fluorescence and luminescence signals were present, aliquots of *E. coli* O157:H7 GFPlux were then mixed with 50% glycerol and stored at −70°C. Prior to the experiments, an aliquot of *E. coli* O157:H7 GFPlux from storage at −70°C was streaked onto an LB agar plate containing 100 μg/ml ampicillin and incubated overnight. A single colony was inoculated into 50 ml of LB broth with 100 μg/ml ampicillin and grown overnight. The overnight culture was used for all the experiments in this study.

Demonstrating the advantages of multiphoton imaging over confocal imaging for resolving the localization of *E. coli* O157:H7 GFPlux in lettuce leaves. A control experiment with lettuce leaves and *E. coli* O157:H7 GFPlux was conducted in order to demonstrate higher spatial resolution with multiphoton imaging than with confocal imaging. *E. coli* O157:H7 GFPlux internalized by vacuum infusion and *E. coli* O157:H7 GFPlux deposited on the leaf surface by spraying were compared as model cases to demonstrate the advantages of multiphoton imaging, as shown in Fig. 1, experiment A. Vacuum infusion is utilized to artificially internalize *E. coli* O157:H7 GFPlux into the mesophyll layer of the leaf, and the process is adapted from a common technique used in *Agrobacterium tumefaciens* plant transformation (18). This approach was selected as a positive control in this study to demonstrate the potential of multiphoton imaging to detect internalized bacteria in intact plant leaves.

Heads of green leafy lettuce (*Lactuca sativa*), a color variation on red leaf lettuce, with an average head length of 20 to 24 cm were purchased from a local supermarket. The outer whorl of the lettuce head was discarded, and the rest of the leaves, except for the heart of the lettuce head, were separated from the head before being washed in deionized water. Leaves that had any evidence of tissue damage or that were not of a size similar to that of the majority of the leaves were discarded. The chosen leaves were dried with paper towels and cut into 1-cm-diameter disks from the leafy portion of the leaves, excluding vascular tissue. For internalization to the mesophyll layer of the leaf, these leaf disks were then submerged into 25 ml of overnight culture of *E. coli* O157:H7 GFPlux, still in LB medium, in 50-ml plastic tubes. The 50-ml tubes were then placed into a sealed vacuum chamber, and the pressure within the vacuum chamber was lowered by a vacuum pump to 25 lb/in^2 for 10 min. After 10 min, the vacuum was immediately released, allowing the *E. coli* O157:H7 GFPlux cells to enter the leaf tissue. The leaves were then removed from the culture, washed three times in 10 ml of 1× phosphate-buffered saline (PBS) buffer in a 50-ml tube for 10 min, and then prepared for imaging. To compare with internalized *E. coli* O157:H7 GFPlux, surface-inoculated *E. coli* O157:H7 GFPlux leaves were also prepared. These leaves were also washed in deionized water, dried with paper towels, and cut into 1-cm-diameter leaf disks. The leaf disks were then sprayed approximately 5 times with a consumer-type sprayer filled with an overnight culture of *E. coli* O157:H7 GFPlux, and then the leaf disks were allowed to dry. Once dry, the disks were prepared for imaging. Both internalized and surface-inoculated *E. coli* O157:H7 GFPlux leaf disks were imaged using the protocol described below.

Experimental design for examining the influence of vacuum cooling on *E. coli* O157:H7 infiltration in leafy greens. In this study, three conditions, i.e., vacuum cooling, leaf side, and surface moisture, were selected to examine the influence of vacuum cooling on the infiltration of *E. coli* O157:H7 in leafy greens. Surface moisture was included as a condition, as additional water can be sprayed on the produce to reduce the loss of product moisture during cooling. Leaf side was chosen due to the differences in surface topology between the adaxial and abaxial sides of the leaf. Each of the conditions selected for the study differed at two levels. For the vacuum cooling condition, the two levels were a control with no cooling and vacuum-cooled samples. For the moisture content, the two levels were high moisture and low moisture. For the leaf side, the two variables were adaxial and abaxial sides of the leaf. A pictorial summary of the study design is depicted in Fig. 1, experiment B. The experimental design of this study was based on a 3-way factorial design of the conditions. The 8 combinations of the three conditions based on the factorial design of experiment were: (i) vacuum cooling, high moisture, and abaxial side; (ii) vacuum cooling, high moisture, and adaxial side; (iii) vacuum cooling, low moisture, and abaxial side; (iv) vacuum cooling, low moisture, and adaxial side; (v) control, high moisture, and abaxial side; (vi) control, high moisture, and adaxial side; (vii) control, low moisture, and abaxial side; and (viii) control, low moisture, and adaxial side. For each of these combinations, two independent repeats were made using multiphoton imaging. The multiphoton-imaging data constituted the primary data set. For each repeat, 3 leaves were prepared for each combination of conditions, and for each leaf, two 1-cm disks were prepared for multiphoton imaging. Furthermore, for each disk, two image stacks (*xy* images stacked in the *z* direction) were acquired. For all the experimental conditions selected in this study, 188 image stacks were acquired as a data set. Each image stack was examined for *E. coli* O157:H7 GFPlux association with stomata and internalization within the leaf. Association with stomata and infiltration were chosen as the dependent variables for statistical analysis for their risk factors of contributing to food-borne illnesses.

Vacuum cooling experiment preparation. Following the experimental design outlined above, whole lettuce leaves were washed and dried. Approximately 10 ml of overnight culture (approximately 10^8 CFU/ml)

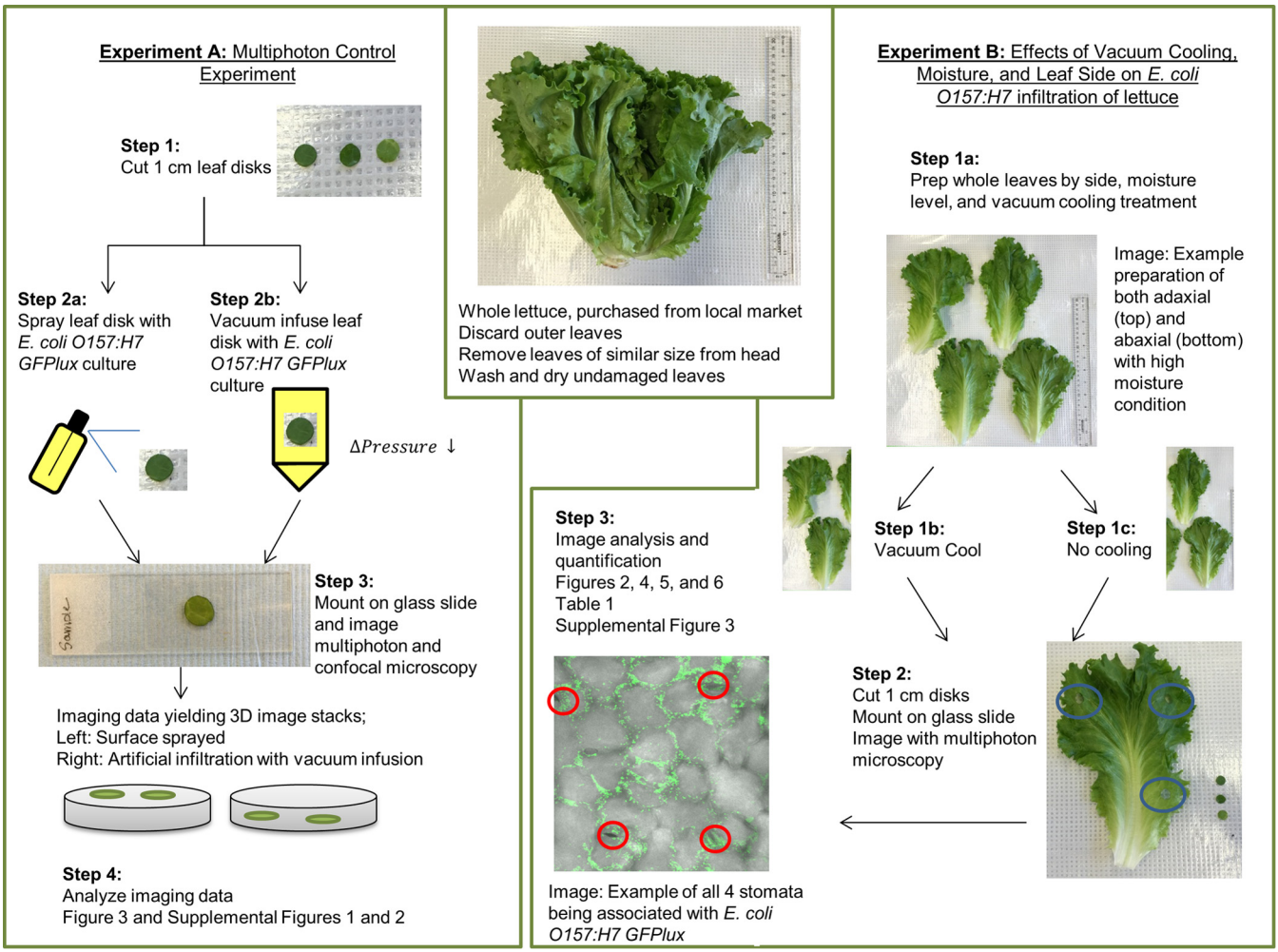

FIG 1 Schematic depicting experimental design for the study. As indicated in the center panel, the whole lettuce head was prepared similarly for both experiments. The outline for the multiphoton-imaging control experiment is detailed for experiment A on the left, showing both the surface-inoculated and artificially infiltrated cases. The experimental outline for the 3-way factorial study on vacuum cooling, moisture, and leaf side is detailed for experiment B on the right. 3D, three-dimensional.

was loaded into a consumer-type sprayer. *E. coli* O157:H7 GFPlux was inoculated by spraying it 5 times evenly on the chosen surface of the lettuce leaf (approximate average surface area, 122 cm^2), depositing approximately 1 ml. Spraying was chosen as an inoculation method to achieve a uniform dispersion of the microbes on the surfaces of lettuce leaves. This approach also mimics certain aspects of the cross-contamination process in which contaminated water may be sprayed on fresh produce during vacuum cooling. Sanitation of the processing water used during cooling and washing has been a subject of significant concern in the fresh produce-processing industry (19–21). In order to determine the average load sprayed onto the leaf disks, leaf disks with surface-inoculated *E. coli* O157:H7 GFPlux were prepared and vortexed in 5 ml of 1× PBS buffer for 10 min immediately following inoculation. After being washed, the leaves were extracted from the washing liquid. The washing liquid was then serially diluted in 1-ml sample sizes, and 100 μl of each serial dilution was plated on the surface of LB agar plates supplemented with 100 μg/ml ampicillin and incubated at 37°C overnight. The colonies were counted by visual inspection and adjusted for sample and washing liquid volumes to determine the numbers of CFU/leaf disk. It was determined that this spraying method deposited an average of 10^6 CFU per 1-cm-diameter leaf disk.

After inoculation, selected leaves for the dry condition were placed in a laminar airflow under lab conditions to speed dry for approximately 60 min. The leaf surface was considered dry if liquid droplets were not detected by visual inspection on the surface of the leaf. Once dry, the leaves were placed in bags for transport. Wet leaves were placed immediately in bags to prevent the evaporation of surface moisture.

For the samples to be treated with vacuum cooling, the whole lettuce leaves were placed in a single layer on a platform in a high-vacuum chamber capable of reaching 27 in. Hg (Department of Biological and Agricultural Engineering, University of California, Davis, CA, USA). A needle thermocouple was placed in one of the leaves and connected to a temperature data logger on the outside. The leaves were vacuum cooled at a vacuum pressure of 685.8 mm Hg for an average of 5 to 7 min to an average temperature of 6 to 8°C. After reaching the average temperature, the vacuum cooling unit was shut off for 1 min, and then the vacuum was released slowly over several minutes. A control set of leaves was not vacuum cooled and was set aside during the vacuum cooling process.

To prepare for multiphoton imaging, two 1-cm-diameter disks were cut from individual leaves and mounted to slides. All disks were cut from similar positions on the leaves. The vascular tissue was excluded from this study due to its extreme variation in thickness, thereby increasing the

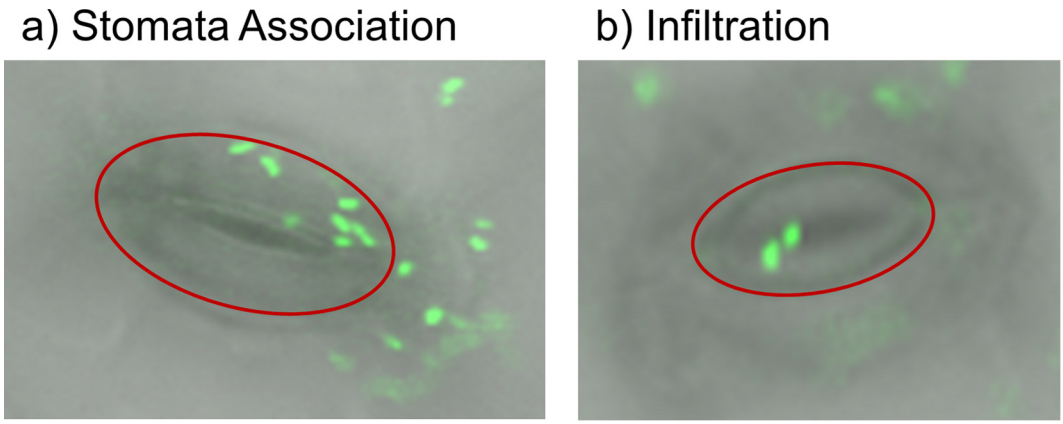

FIG 2 Schematic demonstrating the definitions of stoma association and infiltration used in collecting data for statistical analysis. Representative images were chosen and cropped to highlight examples of stoma association and microbial infiltration. (a) Stoma association of *E. coli* O157:H7 GFPlux at the surface of a lettuce leaf. Each stoma associated with *E. coli* O157:H7 GFPlux was counted as 1. (b) Infiltration of *E. coli* O157:H7 GFPlux below the leaf surface, examined 4 to 8 μm below the surface.

difficulty in imaging. Each leaf disk was placed on a microscope slide, inoculated side up. A coverslip was mounted with tape on either side to prevent movement of the leaf disk or coverslip.

Multiphoton and confocal imaging. A Zeiss LSM 510 upright microscope with a titanium sapphire laser tuned to 880 nm was used in all multiphoton (two-photon)-imaging experiments. An HFT KP 700/488-nm dichroic excitation filter was used to pass wavelengths of >700 nm to the sample and wavelengths of <700 nm, except 488 nm, to the detector. A 500- to 550-nm-bandpass emission filter was used to collect GFP signal. For confocal imaging, the same microscope was used with a 488-nm argon laser, an HFT UV/488/543/633 excitation filter, and the same-bandpass emission filter. All multiphoton images were taken with a 40× differential interference contrast (DIC) water objective, and a 40× oil objective was used for confocal imaging. For each leaf disk, 2 sets of image stacks were acquired. An image stack is a collection of *xy* plane images taken at discrete points on the *z* axis, and all stacks are oriented in the same direction; e.g., the *xy* view is the leaf surface, and the *z* axis moves up and down within the leaf tissue. An individual *xy* image of an image stack will also be referred to as a slice. All image stacks were taken from the top of the leaf surface and imaged at 1-μm slices to 20 to 50 μm below the leaf surface, depending on the selected leaf thickness.

Image analysis and quantification. Each combination of leaf side, moisture, and vacuum treatment had 24 image stacks, with one exception of 20 image stacks for the adaxial side, high moisture, and both vacuum cooling and control leaves. For all the experimental conditions selected in this study, 188 image stacks were acquired as a data set. To quantify the effects of vacuum cooling treatment, leaf side, and moisture level, each image stack was evaluated for its association of *E. coli* O157:H7 GFPlux with stomata and leaf infiltration. The data set was compiled into an Excel spreadsheet for statistical analysis (Microsoft, WA, USA). Each stoma that fit the parameters of association was counted as one. Stoma association is defined as at least one *E. coli* O157:H7 GFPlux cell within the boundaries of the guard cells of the stoma. Infiltration is defined as the cell penetrating the leaf below the level of the surface cell layer. Both definitions are shown in Fig. 2. Representative cases for each of the treatments were chosen and are represented vertically in the *z* direction as *xy* images and as a projection in the *xz* direction (see Fig. 4 and 5).

Statistical analysis. The data generated by image quantification were analyzed with SAS (Cary, NC, USA). The three-way factorial analysis of variance (ANOVA) model for *E. coli* O157:H7 GFPlux association with stomata and infiltration was defined as a function of vacuum cooling treatment, moisture levels, leaf side, and their interaction terms. The full models are presented below:

$$\begin{aligned} \textit{Stoma Association} = {} & \textit{Vacuum Cooling Treatment} \\ & + \textit{Moisture} + \textit{Leaf Side} \\ & + \textit{Vacuum Cooling Treatment} * \textit{Moisture} \\ & + \textit{Vacuum Cooling Treatment} * \textit{Leaf Side} \\ & + \textit{Moisture} * \textit{Leaf Side} \\ & + \textit{Vacuum Cooling Treatment} \\ & * \textit{Moisture} * \textit{Leaf Side} \end{aligned}$$

$$\begin{aligned} \textit{Infiltration} = {} & \textit{Vacuum Cooling Treatment} + \textit{Moisture} + \textit{Leaf Side} \\ & + \textit{Vacuum Cooling Treatment} * \textit{Moisture} \\ & + \textit{Vacuum Cooling Treatment} * \textit{Leaf Side} \\ & + \textit{Moisture} * \textit{Leaf Side} \\ & + \textit{Vacuum Cooling Treatment} * \textit{Moisture} * \textit{Leaf Side} \end{aligned}$$

In addition to the initial analysis, *post hoc* testing of the means via least-squares analysis with Tukey's adjustment was carried out to determine any significance between groups. Significant values ($P < 0.05$) are reported.

RESULTS

Multiphoton imaging of *E. coli* O157:H7 GFPlux on the surface and inside of lettuce leaves. Figure 3 illustrates that multiphoton imaging can detect surface and internalized *E. coli* O157:H7 GFPlux in intact lettuce leaves. The results in Fig. 3a show a combined differential interference contrast (DIC) image and fluorescent images at 0, 10, and 20 μm starting at the leaf surface for both the surface-inoculated and artificially infiltrated samples. For the surface-inoculated case, the combined images show fluorescent signal present on the surface, or at 0 μm. The artificially infiltrated set shows the combined DIC and fluorescent images with fluorescent signal shown in the red circle on the image taken 10 μm below the leaf surface. Additionally, the infiltrated *E. coli* O157:H7 GFPlux cells appear under the middle of a grouping of four stomata, indicative of the random infiltration caused by the vacuum infusion process, with the stomata outlined in red. Figure 3b shows an *xz* projection of the image stacks, which shows a side view of the leaf. The dotted green line shows the break between the epithelial and mesophyll layers in the leaf at approximately 4 μm below the surface. The *xz* projection for the surface-inoculated leaf shows the fluorescent signal at the surface and no significant

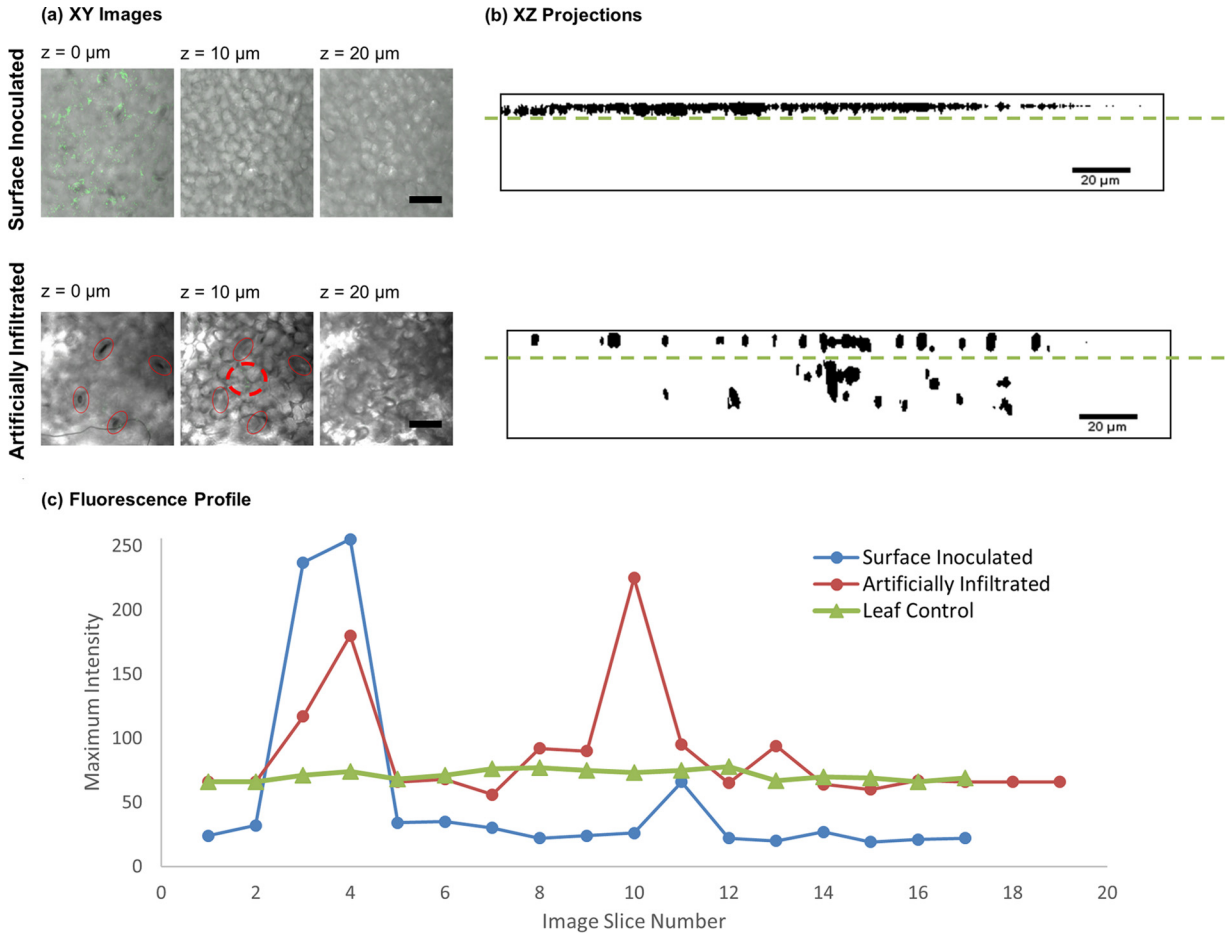

FIG 3 Multiphoton imaging control experiment discerning *E. coli* O157:H7 GFPlux location at the surface of the leaf and artificially infiltrated into the middle of the leaf. (a) Images at 0, 10, and 20 μm are shown to demonstrate the ability of multiphoton imaging to image the surface, middle, and bottom portions of the leaf. In the image at 20 μm for both conditions, the black bar denotes a 50-μm scale. In the surface-inoculated case, *E. coli* O157:H7 GFPlux signal is present only on the leaf surface ($z = 0$ μm). In the artificially infiltrated case, the red ovals outline the locations of the stomata in the 0- and 10-μm images, with the red dotted circle outlining the location of infiltrated bacteria. (b) The *xz* projections show fluorescent signal in the image stack, with the artificially infiltrated image demonstrating clear infiltration of bacteria in the middle of the leaf. The dotted green line indicates the transition between the epithelial and mesophyll cell layers. (c) The maximum intensity for each image in the stack was calculated and then plotted as a function of image slice number. Both the surface-inoculated and artificially infiltrated data reflect the images with the highest intensity, indicating the presence of bacteria in the image slices at the surface (image slices 2 to 4) for both and in the middle (image slice 10) for the artificially infiltrated case.

fluorescent signal in the interior of the leaf. For the *E. coli* O157:H7 GFPlux artificially infiltrated leaf, the *xz* projection shows the fluorescent signal located in the middle of the leaf. Figure 3c shows a graph of the maximum intensity as a function of the image slice. The profile for the surface-inoculated leaf shows a maximum intensity peak of 256 units at slices 2 to 4, which corresponds to the surface of the leaf, indicating the presence of *E. coli* O157:H7 GFPlux at the surface. A much smaller peak at slice 11, which is approximately 10 μm below the leaf surface, indicates some autofluorescence detection from the mesophyll layer of the leaf, which was lower in magnitude than the background signal in the leaf control. It is also important to note that interleaf variations can result in changes in background fluorescence intensity, as illustrated in Fig. 3c. For the *E. coli* O157:H7 GFPlux artificially infiltrated case, the maximum-intensity peak occurs around slice 10, which corresponds to approximately 10 μm below the surface of the leaf. The artificially infiltrated case also shows a smaller peak at the surface around slices 4 and 13. Visual inspection of the stack at slice 4 shows that some microbes remain on the surface despite the surface being washed to remove *E. coli* O157:H7 GFPlux from the leaf. As a comparison, a leaf without inoculated bacteria (leaf control) was included to indicate the background autofluorescence using multiphoton imaging. Further, image spatial resolution and signal contrast in plant tissue are improved with multiphoton imaging compared to those with standard confocal imaging (see Fig. S1 and S2 in the supplemental material).

***E. coli* O157:H7 GFPlux association and infiltration in lettuce leaves under vacuum cooling.** Figure 4 shows representative images for the abaxial side under different moisture and vacuum conditions selected from a set of 96 image stacks. Figure 4a shows cases for high-moisture samples, with (i) a vacuum cooling-treated case, (ii) a control case, and (iii) a control sample that had infiltration. With each case, a combined DIC and fluorescent *xy* image is divided into parts: the surface of the leaf ($z = 0$ μm), 4 μm below the surface, and 8 μm below the surface. Figure 4ai shows a typical vacuum-cooled case, with a relatively even distribution of

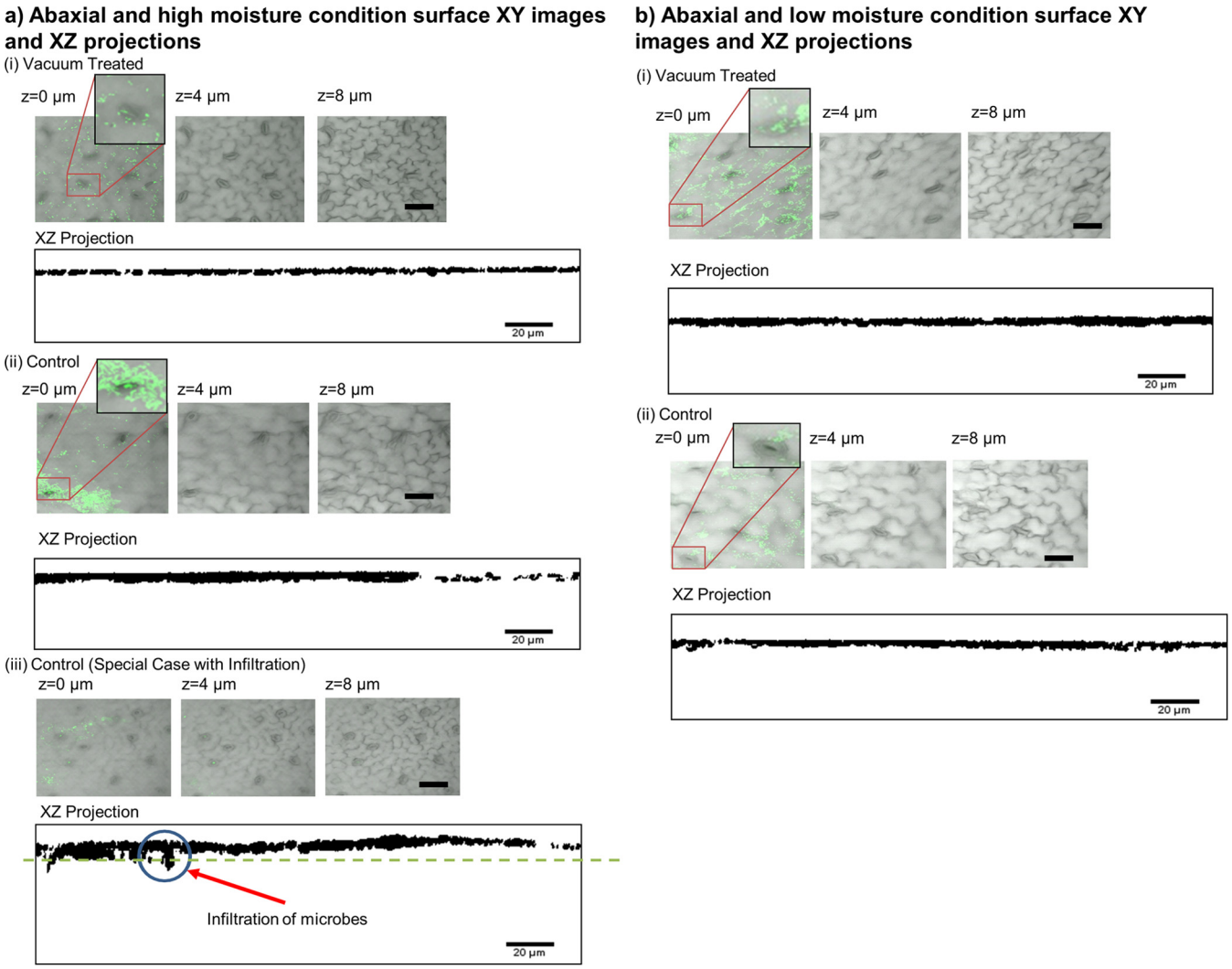

FIG 4 Results for the abaxial side of leaf with moisture and vacuum cooling conditions, with 96 image stacks acquired. Representative images are shown for high moisture (a) and low moisture (b), with 48 image stacks for both conditions. Each case, vacuum cooled (i) and control (ii), shows both surface images at a *z* of 0, 4, and 8 μm and the *xz* projection of the GFP signal in black. (iii) Under the high-moisture condition, an example of infiltration is shown, with a dotted line indicating the end of the epithelial cell layer. The black bar in each of the "$z = 8$ μm" images denotes a 50-μm scale.

signal along the surface of the leaf, as demonstrated in the *xz* projection. Further, no signal is detected below the surface of the leaf. Figure 4aii presents an uneven distribution of fluorescence signal on the surface of a control leaf sample corresponding to the distribution of *E. coli* O157:H7 GFPlux on the leaf surface. Similarly, Fig. 4bi and ii show similar images under the low-moisture condition for the vacuum infiltration and control samples, respectively. In addition to the *xy* images at different *z* heights, an *xz* projection of the image stack is included to demonstrate where the fluorescence signal is located. In all cases, the majority of the signal is at the surface of the leaf, with the exception of the special control case shown in Fig. 4aiii. The infiltrated case in Fig. 4aiii demonstrates natural *E. coli* O157:H7 GFPlux infiltration of the stomata, as seen by the signal present below the epithelial layer within the bounds of the stomatal guard cells above it. Out of 96 image stacks over two independent repeats of data collection, 67 image stacks had at least one stoma associated with *E. coli* O157:H7 GFPlux, and 5 image stacks had at least one instance of *E. coli* O157:H7 GFPlux infiltration. Of the 67 image stacks with at least one instance of *E. coli* O157:H7 GFPlux association with stomata, 37 image stacks were vacuum cooled, and 30 were control samples. Of the 5 image stacks with at least one instance of *E. coli* O157:H7 GFPlux infiltration, 3 were vacuum cooled, and 2 were control samples.

Figure 5 shows representative images for the adaxial side of the leaf. As with the results in Fig. 4, the influence of the moisture level and vacuum cooling parameters on *E. coli* O157:H7 GFPlux localization on leaf surface and infiltration was determined using multiphoton microscopy. Figure 5a shows representative images under the high-moisture conditions selected from the set of 44 image stacks. In the case of Fig. 5ai and ii, the *xz* projection shows an uneven surface distribution of *E. coli* O157:H7 GFPlux with and without vacuum cooling for high-moisture samples. These observations are similar to observations made of the representative cases shown in Fig. 4. Figure 5b demonstrates representative cases under the low-moisture condition, either with vacuum cooling or

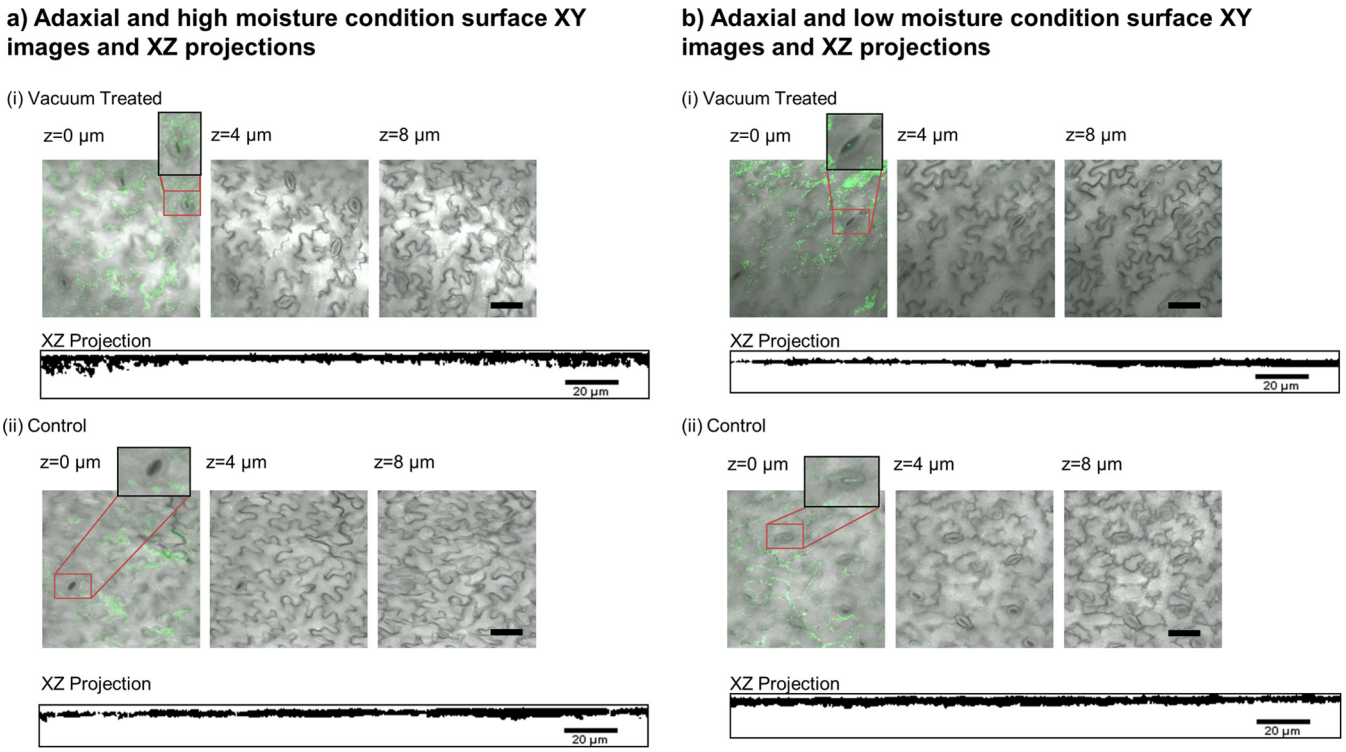

FIG 5 Results for the adaxial side of leaf for moisture and vacuum cooling conditions, with 92 image stacks acquired. (a) Representative cases under high-moisture and vacuum cooling conditions are shown ($n = 44$). (b) Representative cases for low moisture are shown ($n = 48$). Each case for vacuum-cooled and control data shows both surface images at a *z* of 0, 4, and 8 μm and the *xz* projection of the GFP signal in black. The black bar in each of the "z = 8 μm" images denotes a 50-μm scale.

without, selected from a set of 48 image stacks. The surface *xy* image ($z = 0$ μm) and the *xz* projection for Fig. 5bi exhibit uneven distribution of fluorescence signal from the surface *E. coli* O157:H7 GFPlux, similar to the other cases in Fig. 4 and 5a. Similarly, Fig. 5bii shows the majority of the fluorescence signal on the surface. Out of 92 image stacks over two independent repeats of data collection, 86 image stacks had at least one instance of *E. coli* O157:H7 GFPlux association with stomata, and 10 image stacks had at least one instance of *E. coli* O157:H7 GFPlux infiltration. Of the 86 image stacks with at least one instance of *E. coli* O157:H7 GFPlux association with stomata, 46 were vacuum treated and 40 were control samples. Of the 10 image stacks with at least one instance of *E. coli* O157:H7 GFPlux infiltration, 6 were vacuum cooled, and 4 were control samples.

Statistical analysis of changes in *E. coli* O157:H7 GFPlux association with stomata and infiltration under vacuum cooling. The statistical analysis of the ANOVA model for *E. coli* O157:H7 GFPlux association with stomata is summarized in Fig. 6 and Table 1. Among the main effects, which are vacuum cooling, leaf side, and moisture level, only the influence of moisture on the association of *E. coli* O157:H7 GFPlux with stomata was significant ($P < 0.05$). None of the interaction effects were significant

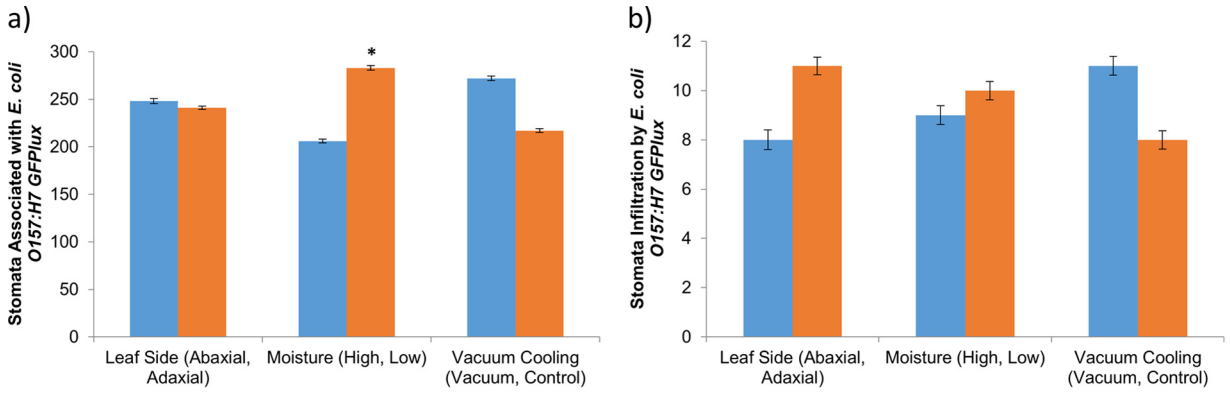

FIG 6 Graphs of the raw data for stoma association and stoma infiltration collected from the 188 image stacks. (a) Leaf side, moisture, and vacuum cooling data are graphed as a function of stoma association with *E. coli* O157:H7 GFPlux. The asterisk indicates a significant difference, as indicated by the statistical model ($P < 0.05$). (b) Leaf side, moisture, and vacuum cooling data are graphed as a function of infiltration of *E. coli* O157:H7 GFPlux.

TABLE 1 Statistical summary of the two variables stoma association and stoma infiltration by *E. coli* O157:H7 GFPlux[a]

Condition(s)	*P* value for:	
	Stoma association	Stoma infiltration
Leaf side	0.8103	0.5657
Vacuum cooling treatment	0.0605	0.5657
High or low moisture	0.0089[b]	0.8481
Leaf side and vacuum cooling treatment	0.3918	0.5657
Leaf side and high or low moisture	0.3551	0.8481
Vacuum cooling treatment and high or low moisture	0.6071	0.0135[b]
Leaf side, vacuum cooling treatment, and high or low moisture	0.2586	0.5657

[a] Stoma association + stoma infiltration = leaf side | high or low moisture | vacuum cooling treatment (see Materials and Methods for more information on the equations).
[b] Significant value ($P < 0.05$).

($P > 0.05$) in influencing the association with stomata. In a *post hoc* analysis, it was determined that the low-moisture condition mean was significantly different from the high-moisture mean for the association with stomata, as shown in Fig. S3 in the supplemental material. Overall, the association of *E. coli* O157:H7 GFPlux with stomata was not influenced by vacuum cooling.

Figure 6 and Table 1 summarize, in addition to the *E. coli* O157:H7 GFPlux association with stomata, the statistical analysis results for *E. coli* O157:H7 GFPlux infiltration. The main effects of vacuum cooling, moisture, and leaf side were not statistically significant ($P > 0.05$) in influencing the infiltration of *E. coli* O157:H7 GFPlux. The vacuum cooling-moisture interaction term was statistically significant ($P < 0.05$). This interaction term can be interpreted as the levels of vacuum cooling being dependent on the levels of surface moisture for the infiltration of *E. coli* O157:H7 GFPlux. *Post hoc* analysis of the means for the significant interaction effect revealed that infiltration is more likely for both vacuum-cooled and noncooled control leaves under low-moisture conditions than under high-moisture conditions ($P < 0.05$), as shown in Fig. S3 in the supplemental material. Further analysis by least mean squares with Tukey's adjustment found that *E. coli* O157:H7 GFPlux infiltration in vacuum-cooled leaves under low-moisture conditions was significantly different from that of noncooled control leaves under low-moisture conditions ($P < 0.05$). Overall, *E. coli* O157:H7 GFPlux infiltration in lettuce leaves was influenced by the interaction between vacuum cooling and moisture levels.

DISCUSSION

Multiphoton microscopy as a tool for microbe imaging in plants. The ability to map microbial location on the surface and within the leaf is critical for establishing the potential infiltration of microbes in lettuce leaves during the vacuum cooling process. Resolution, depth penetration, and low autofluorescence from the plant material are keys to accurately and reliably map microbial distributions in plant tissues. The results from Fig. 3 show that multiphoton imaging can detect *E. coli* O157:H7 GFPlux both on the surface and within the leaves without significant interference from plant autofluorescence. Higher resolution in both white light DIC and fluorescence modes contributes to accurate identification of sample structure and target fluorescence signal; the combination of these modes also allows for accurate spatial mapping of the signal with sample structure, as demonstrated in Fig. S1 in the supplemental material. Data from Fig. S2a and 2b in the supplemental material demonstrate the ability of multiphoton microscopy to resolve both DIC and fluorescence features in a given leaf sample more accurately than confocal microscopy. The line scans of the specific fluorescent areas in the images amply demonstrate the increased signal variation, which allows for increased resolution of the feature as imaged. Additionally, intact plant tissue is by no means ideal for optical imaging, due to its heterogeneous topology of the surface and variation in thickness of the tissue. Both of these factors contribute to increased light scattering and adsorption in the visible wavelengths and can further reduce depth penetration in confocal microscopy. As multiphoton microscopy uses NIR wavelengths, plant surface topology and tissue thickness contribute less to issues of depth penetration, and intact plant leaves may be imaged with minimal sample preparation (13–15). Also, the fluorescent signal within a leaf due to *E. coli* O157:H7 GFPlux is easier to detect due to small amounts of background autofluorescence from the plant tissue.

E. coli O157:H7 infiltration through vacuum cooling has been reported previously (6). To evaluate the increase in general microbial infiltration using the vacuum cooling process, it is essential to detect microbes both on the surface of and inside stomata. In order to demonstrate multiphoton-microscopy capabilities in imaging microbes within an intact leaf, *E. coli* O157:H7 GFPlux, as a model pathogenic microbe, was artificially infiltrated into the leaf by the vacuum infusion process. The vacuum infusion process was selected to prepare a positive control sample in which the bacterial cells were infiltrated into the plant leaves. This approach was selected only to compare the performance of multiphoton imaging with that of conventional confocal imaging. It is important to note that the vacuum infusion process is significantly different from the vacuum cooling process, although both processes are based on vacuum pressure. In the vacuum infusion process, the leaves are submerged into an aqueous solution of microbes, and the microbes are infused into lettuce leaves using a rapid release of vacuum pressure. In a vacuum cooling process, the leaves are not submerged in an aqueous solution. Multiphoton microscopy coupled with superior DIC white light images enables the identification of the position of a microbe within the leaf structure and therefore a determination of whether infiltration has taken place within the leaf.

Vacuum cooling as a risk factor in *E. coli* O157:H7 GFPlux association with stomata and infiltration. For stoma association, vacuum cooling has no significant influence on *E. coli* O157:H7 GFPlux ($P > 0.05$). For the significant moisture effect, an association of *E. coli* O157:H7 GFPlux with stomata is more likely to occur under low-moisture conditions than under high-moisture conditions, as shown in the supplemental material. For infiltration into leaves, vacuum cooling by itself does not influence *E. coli* O157:H7 GFPlux infiltration. The significant interaction term vacuum cooling-moisture indicates that low moisture level and vacuum cooling can significantly contribute to stoma infiltration under the experimental conditions used in this study.

The low-moisture condition common to both stoma association and infiltration indicates that a dry produce state may amplify certain physical and biological effects to induce food safety risk factors. For this study, the low-moisture state was artificially induced by spraying the lettuce leaves with *E. coli* O157:H7

GFPlux culture and then drying the leaves under a laminar airflow. The physical act of drying may move the *E. coli* O157:H7 GFPlux cells into the crevices around the epithelial cells and the guard cells of the stomata, as seen in Fig. 4bi and 5bii, and thus may induce *E. coli* O157:H7 GFPlux association with stomata. For infiltration under vacuum cooling conditions, the drying effect is compounded by the vacuum cooling process to produce the cooling effect. As the pressure is lowered, water can begin evaporating, which draws heat energy away from the product and produces the cooling effect (1). In this process, *E. coli* O157:H7 GFPlux may be moved extremely short distances by the evaporating water, thereby potentially putting it into contact with stomata. Once *E. coli* O157:H7 GFPlux is near the stomata, chemotaxis can occur and the organism can potentially infiltrate the stomata, which can occur post-vacuum cooling while in storage (9, 22, 23). Stomata are involved in gas exchange of molecules, such as oxygen and water vapor, which can attract microbes (22). Microbes, such as *E. coli* and *Salmonella* spp., can infiltrate the mesophyll tissue through the stomatal openings (24). It is possible that an increase in the number of stoma openings can increase the likelihood of *E. coli* O157:H7 GFPlux association and infiltration. Previous studies have evaluated the influence of vacuum conditions on stoma opening (25, 26). The vacuum conditions used in these prior studies were similar to the vacuum cooling conditions used in this study. Using hydraulic conductance measurements, these previous studies reported no significant effect on stomatal restriction or opening (25, 26). Thus, it is unlikely that the mechanical process of vacuum cooling contributes to *E. coli* O157:H7 GFPlux association with stomata by inducing stomata to open. Based on this data set and the possible mechanisms for stoma association and infiltration, maintaining high-moisture conditions in lettuce may decrease the risk of association with stomata or infiltration of *E. coli* O157:H7 GFPlux under the conditions used in this study.

In addition to moisture and vacuum cooling effects on *E. coli* O157:H7 GFPlux association and infiltration of stomata, the relatively high inoculation of *E. coli* O157:H7 GFPlux onto plant leaves may have affected the results. In this study, approximately 10^6 CFU of *E. coli* O157:H7 GFPlux per 1-cm leaf disk was inoculated on the lettuce leaves. Other studies examining bacterium-leaf interactions have inoculated leaf samples at similar high levels of approximately 10^6 to 10^8 CFU/ml (24). The typical microbial load on fresh produce is 10^5 to 10^7 CFU/g of produce, while the pathogen loads are expected to be significantly lower, in the range of 10^1 to 10^3 CFU/g, if present at all on fresh produce (27). The significant effects seen in the association and infiltration models may be inoculation dependent and may disappear when the pathogenic microbial load is lowered to numbers naturally found on plants for food-borne bacterial pathogens. A preliminary experiment using a low inoculation level on lettuce leaves suggests that the significant effects seen in association and infiltration are inoculation dependent (data not shown) and thus might not increase the risk of infiltration.

Conclusions. This study demonstrates the ability of multiphoton microscopy to image microbes in an intact leaf and the application of this imaging approach for evaluating the influence of vacuum cooling on *E. coli* O157:H7 GFPlux infiltration of fresh leafy greens. Multiphoton microscopy is shown to have better resolution and depth penetration than confocal microscopy in both DIC white light and fluorescence images, which are ideal for imaging microbe location within an intact leaf sample. The influence of vacuum cooling, leaf side, and moisture on *E. coli* O157:H7 GFPlux stoma association and infiltration into intact lettuce leaves was studied. Overall, moisture levels, particularly the low moisture level, significantly influenced *E. coli* O157:H7 GFPlux association with stomata ($P < 0.05$). *E. coli* O157:H7 GFPlux infiltration into lettuce leaves was influenced by the interaction of vacuum cooling and moisture levels ($P < 0.05$), and particularly, the low moisture level combined with vacuum cooling increased the risk of infiltration under the experimental conditions in this study. Thus, avoiding low-moisture conditions during vacuum cooling and storage may decrease the risk of infiltration of *E. coli* O157:H7 GFPlux and improve the safety of processing fresh produce.

FUNDING INFORMATION

USDA-NIFA Program Enhancing Food Safety through Improved Processing Technologies (A4131) provided funding to Nitin Nitin under grant number 2015-68003-23411. Center for Produce Safety provided funding to Nitin Nitin under grant number SCB10059.

REFERENCES

1. **McDonald K, Sun D-W.** 2000. Vacuum cooling technology for the food processing industry: a review. J Food Eng **45:**55–65. http://dx.doi.org/10.1016/S0260-8774(00)00041-8.
2. **Cheyney CC, Kasmire RF, Morris LL.** 1979. Vacuum cooling wrapped lettuce. Calif Agric **33:**18–19.
3. **Ozturk HM, Ozturk HK.** 2009. Effect of pressure on the vacuum cooling of iceberg lettuce. Int J Refrig **32:**402–410. http://dx.doi.org/10.1016/j.ijrefrig.2008.09.009.
4. **Rennie TJ, Raghavan GSV, Vigneault C, Gariepy Y.** 2001. Vacuum cooling of lettuce with various rates of pressure reduction. Trans ASAE **44:**89–93. http://dx.doi.org/10.13031/2013.2292.
5. **Sun DW, Zheng LY.** 2006. Vacuum cooling technology for the agri-food industry: past, present and future. J Food Eng **77:**203–214. http://dx.doi.org/10.1016/j.jfoodeng.2005.06.023.
6. **Li H, Tajkarimi M, Osburn B.** 2008. Impact of vacuum cooling on *Escherichia coli* O157:H7 infiltration into lettuce tissue. Appl Environ Microbiol **74:**3138–3180. http://dx.doi.org/10.1128/AEM.02811-07.
7. **Zhang GD, Ma L, Beuchat LR, Erickson MC, Phelan VH, Doyle MP.** 2009. Lack of internalization of *Escherichia coli* O157:H7 in lettuce (*Lactuca sativa* L.) after leaf surface and soil inoculation. J Food Prot **72:**2028–2037.
8. **Taormina PJ, Beuchat LR, Erickson MC, Ma L, Zhang GD, Doyle MP.** 2009. Transfer of *Escherichia coli* O157:H7 to iceberg lettuce via simulated field coring. J Food Prot **72:**465–472.
9. **Melotto M, Underwood W, Koczan J, Nomura K, He SY.** 2006. Plant stomata function in innate immunity against bacterial invasion. Cell **126:**969–980. http://dx.doi.org/10.1016/j.cell.2006.06.054.
10. **Williams RM, Zipfel WR, Webb WW.** 2001. Multiphoton microscopy in biological research. Curr Opin Chem Biol **5:**603–608. http://dx.doi.org/10.1016/S1367-5931(00)00241-6.
11. **Stelzer EHK, Hell S, Lindek S, Stricker R, Pick R, Storz C, Ritter G, Salmon N.** 1994. Nonlinear absorption extends confocal fluorescence microscopy into the ultra-violet regime and confines the illumination volume. Opt Commun **104:**223–228. http://dx.doi.org/10.1016/0030-4018(94)90546-0.
12. **Buschmann C, Lichtenthaler HK.** 1998. Principles and characteristics of multi-colour fluorescence imaging of plants. J Plant Physiol **152:**297–314. http://dx.doi.org/10.1016/S0176-1617(98)80144-2.
13. **Borst J-W, Hink MA, van Hoek A, Visser AJWG.** 2003. Multiphoton microspectroscopy in living plant cells. Proc SPIE **4963:**231. http://dx.doi.org/10.1117/12.477989.
14. **Centonze VE, White JG.** 1998. Multiphoton excitation provides optical sections from deeper within scattering specimens than confocal imaging. Biophys J **75:**2015–2024. http://dx.doi.org/10.1016/S0006-3495(98)77643-X.
15. **Feijo JA, Moreno N.** 2004. Imaging plant cells by two-photon excitation. Protoplasma **223:**1–32. http://dx.doi.org/10.1007/s00709-003-0026-2.
16. **Benediktyová Z, Nedbal L.** 2009. Imaging of multi-color fluorescence

emission from leaf tissues. Photosynth Res **102:**169–175. http://dx.doi.org/10.1007/s11120-009-9498-z.
17. **Karsi A, Lawrence M.** 2007. Broad host range fluorescence and bioluminescence expression vectors for Gram-negative bacteria. Plasmid **57:**286–381. http://dx.doi.org/10.1016/j.plasmid.2006.11.002.
18. **Joh LD, Wroblewski T, Ewing NN, VanderGheynst JS.** 2005. High-level transient expression of recombinant protein in lettuce. Biotechnol Bioeng **91:**861–871. http://dx.doi.org/10.1002/bit.20557.
19. **Beuchat LR, Ryu JH.** 1997. Produce handling and processing practices. Emerging Infect Dis **3:**459–465. http://dx.doi.org/10.3201/eid0304.970407.
20. **Fatica MK, Schneider KR.** 2011. *Salmonella* and produce: survival in the plant environment and implications in food safety. Virulence **2:**573–579. http://dx.doi.org/10.4161/viru.2.6.17880.
21. **Gagliardi JV, Millner PD, Lester G, Ingram D.** 2003. On-farm and postharvest processing sources of bacterial contamination to melon rinds. J Food Prot **66:**82–87.
22. **Zeng W, Melotto M, He SY.** 2010. Plant stomata: a checkpoint of host immunity and pathogen virulence. Curr Opin Biotechnol **21:**599–603. http://dx.doi.org/10.1016/j.copbio.2010.05.006.
23. **Wadhams GH, Armitage JP.** 2004. Making sense of it all: bacterial chemotaxis. Nat Rev Mol Cell Biol **5:**1024–1037. http://dx.doi.org/10.1038/nrm1524.
24. **Kroupitski Y, Golberg D, Belausov E, Pinto R, Swartzberg D, Granot D, Sela S.** 2009. Internalization of *Salmonella enterica* in leaves is induced by light and involves chemotaxis and penetration through open stomata. Appl Environ Microbiol **75:**6076–6162. http://dx.doi.org/10.1128/AEM.01084-09.
25. **Nardini A, Tyree MT, Salleo S.** 2001. Xylem cavitation in the leaf of *Prunus laurocerasus* and its impact on leaf hydraulics. Plant Physiol **125:**1700–1709. http://dx.doi.org/10.1104/pp.125.4.1700.
26. **Sack L, Melcher PJ, Zwieniecki MA, Holbrook NM.** 2002. The hydraulic conductance of the angiosperm leaf lamina: a comparison of three measurement methods. J Exp Bot **53:**2177–2184. http://dx.doi.org/10.1093/jxb/erf069.
27. **Francis GA, Thomas C, O'Beirne D.** 1999. The microbiological safety of minimally processed vegetables. Int J Food Sci Technol **34:**1–22. http://dx.doi.org/10.1046/j.1365-2621.1999.00253.x.